BUTTERWORTH HEINEMANN

Polymer Vol. 36 No. 12, pp. 2323–2330, 1995

0032-3861/95/$10.00 + 0.00

polymer papers

Morphologies of semi and full interpenetrating polymer networks by nuclear magnetic resonance relaxation times

Nathalie Parizel*, Guy Meyer and Gilbert Weill
Institut Charles Sadron (CRM-EAHP), CNRS-ULP Strasbourg, 6 rue Boussingault, 67083 Strasbourg Cedex, France
(Received 9 March 1994; revised 6 September 1994)

Full and semi interpenetrating polymer networks, IPNs, formed with a network of polyurethane (PU), and either a crosslinked poly(methyl methacrylate), PAc, or a linear polystyrene, PS, were synthesized with the aim of obtaining homogeneous materials. As already shown in a previous paper, the degree of phase dispersion in such materials depends on the synthesis method. The purpose of the n.m.r. investigations is to estimate the degree of mixing of the polymer in such networks, together with the synthesis parameters. The n.m.r. lineshape evolution of the PU/PAc IPNs with temperature allowed us to conclude that the PAc and PU networks are more intimately mixed in the sequential mode. In this paper, the measurements of the spin-lattice relaxation times in the rotating frame and the Goldman–Shen experiment are used to confirm previous results, and to give an estimation of the degree of mixing of the two networks in the matrix and of the size of the inclusions of PS in the simultaneous IPN. Following the same protocol, different semi-1 IPNs of PU/PS are examined in order to relate the amount of PS added to the reaction medium with the degree of advancement of the phase separation. Nodules of pure PS are seen for some samples but they do not correspond to those observed by SEM.

(Keywords: nuclear magnetic resonance; relaxation times; interpenetrating polymer networks)

INTRODUCTION

Interpenetrating polymer networks, IPNs, are a special type of polymer blend, in which the two polymers are intimately mixed in their network form[1]. However, the two T_gs usually observed indicate that mixing does not take place at a molecular level, as suggested by the definition of an IPN, and a two-phase morphology is therefore obtained[2].

Since IPNs consist of crosslinked polymers, their morphology is quite complicated, and no general laws have yet been established that correlate synthesis and morphology with the ultimate properties.

Recently, we undertook a solid-state ^{1}H n.m.r. lineshape investigation[3] on PU/PAc [polyurethane/crosslinked poly(methyl methacrylate) (PMMA)] IPNs which differ only in their mode of synthesis: in the *in situ* seqIPNs, the elastomeric network, PU, is formed first, and then the rigid crosslinked PMMA (PAc): in such IPNs, the existence of an initial network impedes gross phase separation in the final material. In the second type, the *in situ* simIPNs, the synthesis of both networks is initiated at once and proceeds to completion more or less simultaneously, so that bigger domains may form, as there is no topological restriction from an already present structure. Different morphologies observed by transmission electron microscopy confirm these assumptions[4]. Our recent studies were based on the evolution of the n.m.r. lineshape of these IPNs with temperature. The changes in mobility of the components in the IPNs, when compared with the individual networks, correspond to interactions between these components. The more drastic changes for the seqIPN indicate stronger interactions between the two components. These experiments allowed us to conclude that the PAc and PU networks are more intimately mixed by a sequential preparation mode.

The spin-lattice relaxation time (T_1, $T_{1\rho}$) measurements may also give some insight into the domain size because of the presence of the spin diffusion in solids, that is, the transport of nuclear spin magnetization. It acts as an averaging process causing closely adjacent phases with different intrinsic relaxation times to give a common averaged value, and is thus another possible approach to estimate the degree of phase interpenetration in IPNs. Spin diffusion is also the basis of the Goldman–Shen experiment. A magnetization gradient is created by allowing complete dephasing of the magnetization associated with the phase with the short T_2, that is the rigid phase, whilst preserving the long T_2 magnetization, that of the PU elastomer network. The proximity of the phase with the short T_2 and the elastomer is then studied by monitoring the diffusion of the magnetization from the elastomer back into the rigid phase.

* To whom correspondence should be addressed

Unfortunately, the values of T_1 were found to be nearly identical for PU and PAc over the whole temperature range. In contrast, the spin-lattice relaxation times are substantially different for PS and PU, so that it seemed interesting to explore them for PU/PS semi-1 IPNs, the phase separation of which had been previously examined[5]: according to the synthesis conditions used, domains of various sizes appeared on the SEM pictures, embedded in a finely dispersed PU/PS matrix. At first sight, these domains were thought to contain only PS, an assumption which remains to be corroborated by other techniques.

We present first the results concerning the relaxation times T_1 and $T_{1\rho}$ for the PU/PS semi-1 IPNs, and the use of the Goldman Shen sequence to obtain an approximate domain size. Second, the results of the n.m.r. lineshape studies on PU/PAc IPNs are compared with those obtained after the $T_{1\rho}$ and the Goldman–Shen experiments.

EXPERIMENTAL

Materials

The materials and their descriptions are listed in *Table 1*. The poly(oxypropylene glycol)s (POPG) and the methacrylic monomers were dried over molecular sieves but not otherwise purified. Styrene was vacuum distilled twice. The other materials were used as received.

Synthesis

Two types of materials were prepared, namely PU/PS semi-1 IPNs, and PU/PAc IPNs. In each case, PU was prepared under stoichiometric conditions, that is $K = [NCO]/[OH] = 1.07$.

PU/PS *in situ* Seq semi-1 IPNs, containing 30 wt% of PU (i.e. 36% of PU ^{1}H), were synthesized. Reactants: Desmodur N, POPG 4000, styrene, AIBN, OcSn, and eventually homopolystyrene. The polymerization of styrene is started by heating the medium at 342 K, following a period of 2 h at room temperature during which the polyurethane network forms completely. Various small quantities of homopolystyrene (PS_a) were dissolved in the initial reaction mixture; despite the introduction of PS_a, the medium remained homogeneous and transparent at this stage. The T_g values are 220 K and 370 K for the PU and the PS components, respectively.

The PU/PAc IPNs containing 25 wt% of PU (i.e. 27% of PU ^{1}H), were prepared by the *in situ* procedure developed in our laboratory[6]. The reagents (Desmodur L, POPG 2000, MMA, TRIM and AIBN) were mixed together and poured into a glass mould after addition of 1 wt% OcSn. Two different IPNs were synthesized: the first IPN, called *in situ* sequential, was made by keeping the mould at room temperature and in the absence of light up to the gelation of polyurethane, and then transferring it to an oven at 333 K; the second IPN, called *in situ* simultaneous, was obtained by heating the mixture at 333 K immediately after filling up the mould. Both IPNs were annealed for one night at 348 K and for 3 h under vacuum at 393 K; their T_g values are 237 K and 403 K for the PU and PAc components, respectively.

Measurements and mathematical treatment

N.m.r. measurements were carried out on a Bruker SXP spectrometer operating at 60 MHz (^{1}H). The resonance field is monitored with a field frequency lock (Drush, n.m.r. gaussmeter and regulation unit TAO2) within 2 μT. The free induction decay (f.i.d.) signal, following a $\pi/2$ pulse of 4 μs generated by a Hewlett Packard pattern generator 8175A, is digitized with a 12-bit LeCroy 6810 (accuracy 1/2000) at the fastest sampling rate of 5 MHz, and finally averaged and treated on an IBM PC personal computer. Numerical computations are performed in the ASYST language.

Measurements of the hydrogen spin-lattice relaxation times T_1 at 60 MHz were performed by the inversion-recovery sequence. For the spin-lattice relaxation in the rotating frame, $T_{1\rho}$, the sequence given in *Figure 1a* was

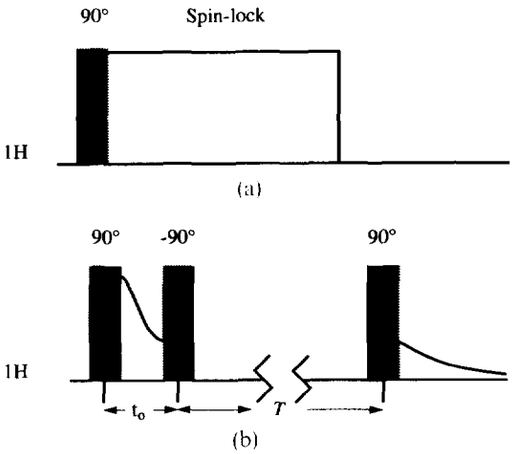

Figure 1 (a) N.m.r. sequence for spin-lattice relaxation measurement in the rotating frame. (b) N.m.r. Goldman–Shen sequence

Table 1 Materials

Material	Description	Supplier
Desmodur L75	1.1.1-Trimethylolpropane/toluene diisocyanate adduct containing 25% ethyl acetate by weight; density: 1.17 g ml^{-1}; 3.06 NCO kg^{-1}	Bayer AG
Desmodur N	Aliphatic adduct based on hexamethylene diisocyanate; density: 1.07 g ml^{-1}; 5.2 NCO kg^{-1}	Bayer AG
POPG 2000	Poly(oxypropylene glycol), M_n = 1990 g mol^{-1}; density: 1.0 g ml^{-1}; hydroxyl content: 1.06 mol kg^{-1}	Arco Chemicals
POPG 4000	Poly(oxypropylene glycol), M_n = 4000 g mol^{-1}; density: 1.02 g ml^{-1}; hydroxyl content: 0.52 mol kg^{-1}	Arco Chemicals
Kosmos 29	Stannous octoate, stabilized; tin content: 29.1% by weight; density: 1.25 g ml^{-1}	Goldschmidt
MMA	Methyl methacrylate; inhibitor; 15 ppm methylethylhydroquinone	Merck
TRIM	1.1.1-Trimethylolpropane trimethacrylate; inhibitor: 100 ppm methylethylhydroquinone	Degussa
S	Styrene; inhibitor: ter-butyl pyrocatechol: 20 ppm	Merck
PS_a	Anionic polystyrene; $M_n \approx 105\,000$ g mol^{-1}; polydispersity index: < 1.1	This laboratory
AIBN	2,2'-Azobisisobutyronitrile	Merck

used. Most of the relaxation curves (T_1 and $T_{1\rho}$) appear multiexponential. The general integral equation describing multiexponential relaxation is:

$$y(t_i) = y_i = \int_a^b s(T)\, e^{-t_i/T}\, dT \quad i = 1, 2, \ldots, N \qquad (1)$$

where the N data y_i are measured at times t_i, and $s(T)$ is the unknown amplitude of the spectral component at the relaxation time T. T represents either T_1 or $T_{1\rho}$. The limits on the integral are restricted to the finite values a and b which are chosen so as to contain the values of T expected for the system being analysed which is contained in the sampled t_i interval. The kernel of equation (1) is $e^{-t_i/T}$, which is the amount that a signal with relaxation time T has decayed by measurement time t_i. For computer implementation, equation (1) must be discretized:

$$y_i = \sum_{j=1}^{M} s_j\, e^{-t_i/T_j} \qquad (2)$$

with M being the number of different relaxation times T_j. Thus equation (1) can be written as:

$$y_i = \sum_{i,j} A_{ij} s_j \quad \text{with } A_{ij} = e^{-t_i/T_j} \qquad (3)$$

Two different numerical approaches are used to determine the relaxation time distributions[7]. First, a discrete spectrum composed of delta functions at a few isolated and widely different relaxation times (ASYST algorithm) is tried[8]. Second, a continuous distribution of relaxation times by inverse Laplace transform is computed (CONTIN package)[9,10]. Note that the distribution of relaxation rates obtained is plotted on a logarithmic x-axis and thus the areas of the different peaks are not directly comparable. This latter treatment is adopted when several relaxation times are too close to each other (a factor of 3 or less), so that the discrete multiexponential decomposition is badly defined. Furthermore, our relaxation experiments are performed on complex, intimately mixed polymer blends, which may lead to many very similar values.

Numerical instability is then overcome by additional constraints, such as bounding the solutions. We imposed $s_j > 0$ and $T_j > 0$ which usually leaves a resolution with three to four parameters.

The Goldman–Shen sequence[11] allows the study of systems that have two sufficiently different spin–spin relaxation times T_2; M_s designates the magnetization of the spins having the slowest relaxation and M_f the fastest spin–spin relaxation. The aim of the Goldman–Shen sequence is to induce the reappearance of M_f by spin diffusion in order to estimate the size of the domains of slow relaxation. The sequence is illustrated on *Figure 1b*. The time t_0 is chosen in such a way that M_f has totally disappeared but that a sufficient amount of M_s is left. The $-90°$ pulse after t_0 creates a spin temperature difference between the two systems associated with M_s and M_f. The magnetizations become longitudinal. M_f is zero and its associated spin temperature is close to infinity while the spin temperature T_s associated with M_s is finite. The spin temperature[12] of the lattice, T_L, in the intense magnetic field B_0 is related to the magnetization M_I by:

$$\vec{M}_I = \frac{N_I \gamma_I^2 \hbar^2 \vec{B}_0}{4kT_L} \qquad (4)$$

where N_I is the number of spins, $\hbar$ is Planck's constant and γ the gyromagnetic ratio. When two different spin temperatures T_s exist within the sample, the spin-diffusion phenomenon occurs. In solids, spin diffusion phenomena have also to be taken into account during spin-lattice relaxation time measurements. Effectively, during the inversion recovery sequence (180°, t, 90°) when two spin-lattice relaxation times are different enough in a sample, for certain values of the delay t, the nuclei with short relaxation time will have completely recovered their equilibrium magnetization: they will be 'cold', while those with a longer relaxation time will not have wholly relaxed: they will be 'hot'[13]. An equilibrium between the two spin temperatures is reached from hot spins to cold ones by spin diffusion. The same process takes place during $T_{1\rho}$ measurements for appropriate spin-lock times if different spin-lattice relaxation times in the rotating frame exist. Thus, when two or more different spin temperatures exist, the associated spin populations tend towards an internal equilibrium by mutual spin flips[14]. The flip-flop probability is proportional to the strength of the dipolar interaction between spins and this is an energy-conserving or spin–spin relaxation time type of process termed spin diffusion[15]. It has been shown that in a regular lattice with lattice constant a, the spin diffusion coefficient due to dipolar spin flip is given by:

$$D = 0.13 a^2 (M_2)^{1/2} \qquad (5)$$

where M_2 is the second moment of the n.m.r. lineshape. Since, for disordered systems like polymers, the diffusion constant is an ill defined quantity, a numerical value can only be estimated and the hydrogen van der Waals radius was used for a. In addition to the internal equilibrium between the two spin systems, both populations tend to be in equilibrium with their surroundings by exchange of energy between the spin and lattice systems and it is a T_1 or spin-lattice process. Spin diffusion and spin lattice relaxation coexist during the time of measurement. The nuclear spin magnetization can diffuse between the two regions in a time of the order of the longer relaxation time[16–19]. Assuming three-dimensional diffusion, the root-mean-square distance, $\langle r^2 \rangle^{1/2}$, is given by:

$$\langle r^2 \rangle^{1/2} \simeq (6DT_i)^{1/2} \qquad (6)$$

where T_i is the relaxation time[20]. If one considers that the spin-lattice relaxation time in the laboratory frame is of the order of 1 s and the spin-lattice relaxation time in the rotating frame is ~ 10 ms, the associated lengths are of the order of 100 and 10 Å[21]. Roughly speaking, two spin systems possessing different T_1 values will seem to relax with only one T_1 is their populations are less than 100 Å apart.

Under the conditions of the Goldman–Shen sequence, the spin diffusion levels, the two spin temperatures and M_f will reappear depending on the delay time τ. The recovery factor $R(\tau)$ is calculated from the increasing fraction of fast component in the lineshape analysis of the time-dependent signal:

$$R(\tau) = \frac{\%\, M_f(\tau)}{\%\, M_f(\text{equilibrium})} \qquad (7)$$

The T_1 contribution is negligible in the case of $\tau \ll T_1$, but it can be taken into account using:

$$M(t) = M_0(1 - e^{-t/T_1}) \qquad (8)$$

The time evolution of $R(\tau)$ is governed by the size, shape and spin diffusion coefficient D_s of the domains with the slowest spin–spin relaxation. Because of the symmetry of the polymeric networks, we associate our systems to a three-dimensional network. In the case of a biphasic structure with instant spin diffusion in hard domains on one hand and slow diffusion in soft domains on the other hand, Cheung and Gerstein[22] have developed a mathematical model relating the magnetization recovery to the diffusion length:

$$R(\tau) = \frac{6}{(\pi)^{1/2}} \sqrt{\frac{D_s \tau}{\bar{b}^2}} \quad \text{for } \tau \ll \bar{b}^2/D_s$$

and

$$R(\tau) = 1 - \sqrt[3]{\frac{\bar{b}^2}{\pi D_s \tau}} \quad \text{for } \tau \gg \bar{b}^2/D_s \qquad (9)$$

with $\bar{b}$ being the mean width of the domain having the slowest spin–spin relaxation. When the spin diffusion coefficient D_s and the average shape of the 'slow relaxation' domain are known, $\bar{b}$ can be determined directly from the initial slope of the $R(\tau)$ vs. $\tau^{1/2}$ plot. Otherwise, if the f.i.d. is composed of three or more different spin–spin relaxation curves, the recovery of the magnetization associated with the shorter T_2 will be done, in a Goldman–Shen experiment, via the magnetization relating to the intermediate T_2. In this case, because the spin diffusion coefficient is different in the separate phases, the recovery curve will be more complex.

RESULTS AND DISCUSSION

30/70 PU/PS semi-1 IPNs

Semi-1 IPNs based on crosslinked PU and linear PS are transparent if prepared by the *in situ* sequential synthesis mode, i.e. PU is completely formed before the onset of styrene polymerization[5]. In this case, gross phase separation is prevented by the already existing network. If very small amounts of polystyrene (PS_a) are now added to the initial mixture of reactants, light transmission (*Figure 2*) decreases, due to turbidity appearing at shorter and shorter times with increasing PS_a content (or molecular weight); with more than 0.5% PS_a, the reaction medium becomes milky right at the beginning of PU formation. Optical microscopy observations reveal nodules, the diameter of which, amongst other parameters, increases with the amount of PS_a present (*Table 2*). The morphology of these nodules could be seen in more detail by SEM[5]; they are surrounded by a shell richer in PU than the overall 30 wt% of the semi-1 IPN. However, it could not be determined by this method whether the nodules consisted of pure PS or of PS containing some PU. N.m.r. investigations were undertaken in order to yield more details about the matrix but, unfortunately, no more information about the nodules was obtained.

As explained above, the degree of homogeneity of a composite system may be evaluated in different ways: first, by measuring the spin-lattice relaxation times in the laboratory frame (T_1) and in the rotating frame ($T_{1\rho}$)[23], taking into account the spin diffusion; second, by considering the sequences using the spin diffusion directly, which allows the magnetization transfers between the domains to be followed according to the diffusion time imposed.

The T_1 relaxation curves of the neat components, and of semi-1 IPNs with various PS_a contents, have been examined. The rate distributions of PU and PS (*Figure 3*) each consist of one sharp peak. However, in the PU

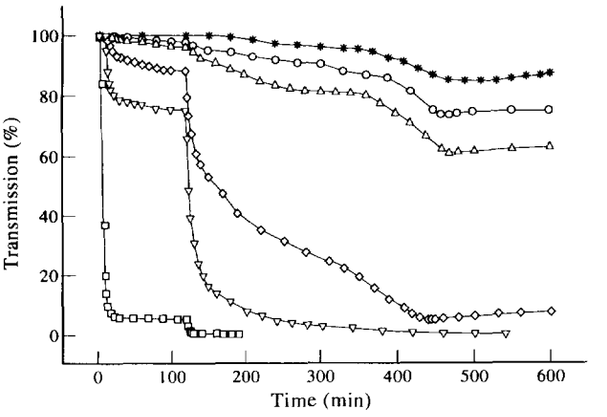

Figure 2 Light transmission curves during formation of 30/70 PU/PS semi-1 IPNs in the presence of various amounts of homopolystyrene, $M_n(PS_a) = 105\,000$ g mol^{-1}: 0 wt% (*), 0.01 wt% (○), 0.02 wt% (△), 0.05 wt% (◇), 0.1 wt% (▽), 0.5 wt% (□)

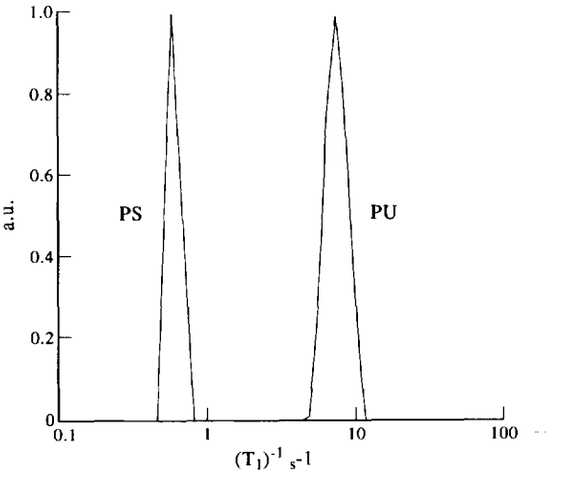

Figure 3 Distribution of spin-lattice rates in the laboratory frame for PS and PU

Table 2 Light transmission and diameter of the nodules as a function of the concentration of homopolystyrene PS_a in the initial mixture

	PS_a (wt%)						
	1.4	0.5	0.1	0.05	0.02	0.01	0
Light transmission (%)	0	0	0	7.2	62.3	74.6	86.8
Diameter (μm)	6.70	4.91	3.91	1.87	0.78	–	0.70

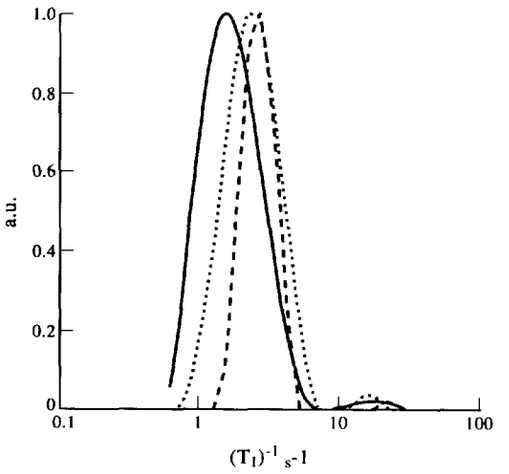

Figure 4 Distribution of spin-lattice rates in the laboratory frame for semi-1 IPNs with various amounts of PS_a: without PS or 0.02 wt% (– –); 0.5 wt% (· ·); 1.4 wt% (——)

network, species of quite different mobilities coexist, such as crosslink points, elastic chains and dangling chains (network defects) and more than one peak would therefore be expected: in fact, the spin diffusion explains this unique peak. *Figure 3* also shows that PS and PU have quite different relaxation times, the latter being about ten times faster.

The semi-1 IPN without PS_a in *Figure 4* (dashed line) yields two peaks, the areas are respectively 93.5 and 6.5%, taking into account the logarithmic scale of the x-axis. The main peak, situated between that of the pure components, is due to their intimate blend. The other one appears beyond the peak of PU, and relaxes therefore even faster than the elastomer. The f.i.d. of a semi-1 IPN is composed of the signal of the PS (Gaussian function with $M_2 = 8\ G^2$) and that of the PU (Weibull function with $T_2 = 500\ \mu s$). Because those signals are sufficiently different and because, due to long delays in the T_1 experiments, only the fastest part of the f.i.d. remains, the peak of fast T_1 relaxation rates is attributed to some PU regions. It corresponds to soft domains of PU not coupled to the remaining sample.

By adding various amounts of PS_a, the two peaks remain (*Figure 4*), and are related to the same species as above. The area of the small peak varies from 6.5 to 11%, when the amount of PS_a increases from 0.02 to 1.4%. With only 0.02%, the relaxation plot remains the same as in the absence of PS_a, which implies that the morphology of the material is not changed on the present observation scale.

The main peak in *Figure 4* is also affected by the addition of PS_a: when the amount of PS_a increases, the peak broadens and is shifted towards the pure PS peak. The broadening can be attributed to two distinct factors. First, it can be induced by the spin diffusion phenomenon itself; but the appearance of a gradient of compositions compared with the initial PU and PS amounts leads also to such a broadening. The broadening towards long T_1 indicates that with more PS_a, more isolated PS is present, either by an increase of PS-enriched regions, or because these regions are less numerous but bigger. However, it is also obvious from these figures that pure PS domains of over 100 Å do not exist except in the samples with 0.5 and 1.4% PS_a, which are the only ones to include the domain of the relaxation rates of the pure PS. The n.m.r. results were compared with those obtained by optical microscopy (*Table 2*), which show a continuous increase of the diameter of the nodules with PS_a content. Under the same conditions a progressive shift of the main peak toward the peak of pure PS is observed in T_1 measurements and is associated with an increase of the size of the PS-enriched regions. Nevertheless, such domains represent only a little of the whole material, because of the very small area corresponding to the pure PS peak compared to the entire distribution after deconvolution. They cannot directly be associated with the nodules of several micrometres in size, shown by optical microscopy and representing about 8% by volume of the sample.

In brief, through T_1 investigations, one may conclude that semi-1 IPNs (% $PS_a \leqslant 0.02$) are homogeneous materials at a scale of 100 Å. With higher PS_a contents, PU-enriched and PS-enriched phases exist, and for $PS_a \geqslant 0.5\%$, even pure PS domains of at least 100 Å are present, as indicated by the broadening towards the high relaxation times. These considerations point to an increase of total volume of PS-enriched regions with increase of PS_a amount.

This is a first result concerning the degree of homogeneity of the different semi-1 IPNs, but observation of the structure on a smaller scale requires shorter n.m.r. relaxation times, i.e. $T_{1\rho}$. These have been calculated after an ASYST treatment: the decay of the PU network has two distinct values: $T_{1\rho} = 16$ ms, associated with the elastic chains (91%) and $T_{1\rho} = 1.3$ ms for the crosslink points (9%). For the PS, the $T_{1\rho}$ value is 1.8 ms. In *Figure 5*, the inverse Laplace transforms of the relaxation curves are drawn for PU and PS (dotted lines) and for the semi-1 IPN without PS_a (continuous line); the curves are the same up to 0.5% PS_a. In *Figure 6*, the semi-1 IPN with 1.4% PS_a is reported, again with the curves of PS and PU. In *Figure 5*, the distribution of the semi-1 IPN is quite large; it partly overlaps both pure components with all the intermediate compositions. In contrast, the distribution of the semi-1 IPN with 1.4% PS_a shows two peaks; the higher corresponds to the

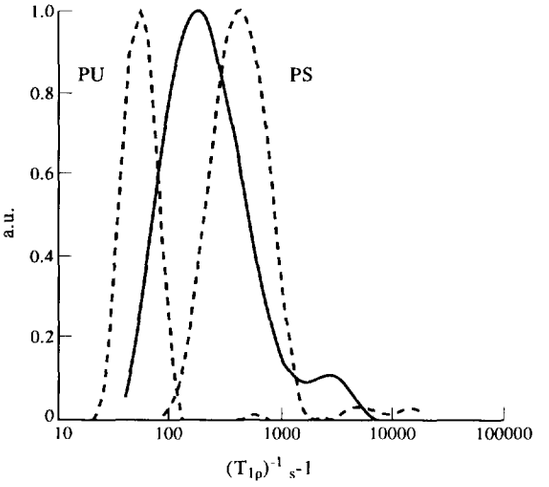

Figure 5 Distribution of spin-lattice rates in the rotating frame for PU and PS (– –), and for a semi-1 IPN with 0 wt% PS_a (——)

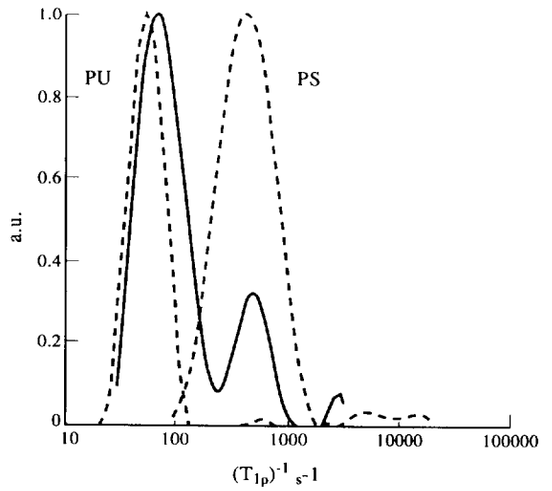

Figure 6 Distribution of spin-lattice rates in the rotating frame for PU and PS (--), and for a semi-1 IPN with 1.4 wt% PS_a (——)

elastic PU chains; the second represents the PS and the PU crosslinks. Therefore, on a scale of 10 Å, domains of both pure PS and pure PU exist, together with mixed domains, for semi-1 IPNs containing up to 0.5% PS_a. For higher PS_a contents, it is clear that less mixed domains are present.

Experiments based on the Goldman–Shen pulse sequence were performed in order to try to detail the structure even further. First, we summarize the results obtained by f.i.d. analysis. The f.i.d. signal of the PS is fitted by a Gaussian function with $M_2 = 8\ G^2$. For the PU, we chose a Weibull function of coefficient 1.2 with a spin–spin relaxation time of 500 μs. The f.i.d. signal of the semi-1 IPNs is nearly the superposition of these two functions with the relative fractions associated with the number of protons of PS and PU. According to these results, the value $t_0 = 100\ \mu s$ of the Goldman–Shen sequence has been chosen so that the magnetization of the first part (PS) has relaxed, whereas the slower relaxing spins (PU) keep a part of their magnetization and may transfer it to the faster one. In this way, and with an increasing τ, the fast relaxing part of the f.i.d. will reappear. *Figure 7* shows the recovery factor $R(\tau)$ as a function of $\tau^{1/2}$ for four semi-1 IPNs with various amounts of homopolystyrene. The curves show two different spin diffusion rates. The first, which is faster, allows from the initial slope, and after the *a priori* choice of both a model (here the Cheung and Gerstein model[22]) and a value for D, the determination of the sizes of the domains with the longest relaxation time T_2. To a good approximation, D is inversely proportional to T_2, and by assuming a D value of $5 \times 10^{-12}\ cm^2\ s^{-1}$ for a rigid lattice with a T_2 of 10–20 μs, an elastomeric phase with a T_2 of 500 μs will have a D value of $2 \times 10^{-13}\ cm^2\ s^{-1}$ (ref. 20). The values of the mean width of the domains having the slowest spin–spin relaxation are reported in *Table 3*. When the amount of PS_a increases, the mean width, b, of the component with the longest spin–spin relaxation time (PU) increases. The variation of b is small and its value, around 100 Å, indicates the presence of a phase where PU and PS are mixed at this scale. The second spin diffusion rate, which is slower, does not allow the total recovery factor to be reached. The maxima of the recovery factor, $R(\tau)_{max}$, for the experiment are reported on *Table 3*. The decrease of $R(\tau)_{max}$ by increasing the amount of PS_a can be explained by an increase of either the size of the PS domains or of the PU ones. Indeed, if the PS phases become larger than the length of the spin diffusion through PS, the spins of the core of such domains cannot be reached by the flip-flop process, and if some PU regions are bigger than the length of the spin diffusion, the entire magnetization cannot be transferred. Because the T_1 measurements give no evidence of significant amounts of large PS domains, one may conclude that the samples contain PU domains larger than 300 Å and that they become bigger when the amount of PS_a increases.

The phase separation is more important with increasing PS_a content, and at a finer scale ($T_{1\rho}$) the results show that with more than 0.5 wt% PS_a, nodules of pure PS exist. It appears that the same heterogeneities are not seen with the n.m.r. technique or by optical microscopy. Inclusions of 100 Å in size are not visible by optical microscopy, and the nodules of several micrometres which represent about 8% of the sample (in volume for the semi-1 IPN with 0.5% of PS_a) are not clearly shown by n.m.r.

25/75 PU/PAc IPNs

For the present PU and PAc homonetworks, a coincidence of the relaxation times T_1 was found to exist for the temperature range under consideration[3], so that their combination as IPNs should yield essentially the same result whatever the morphology obtained by the different synthesis modes. As the T_1 measurements failed

Table 3 Mean width (b) of the longest spin–spin relaxation time component and maximum of the recovery factor ($R(\tau)$) for various amounts of PS_a

	PS_a content (%)			
	0	0.02	0.5	1.4
b (Å)	57	60	78	93
$R(\tau)_{max}$	0.70	0.63	0.58	0.39

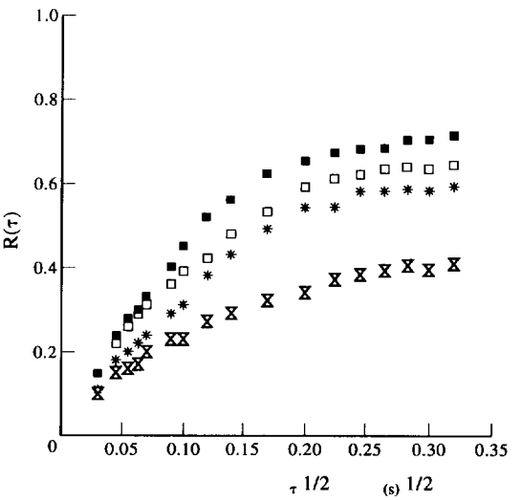

Figure 7 Recovery factor of the magnetization for PS resonance, $R(\tau)$, in a Goldman–Shen experiment after a preparation period of 100 μs as a function of the spin diffusion time τ, for various amounts of PS_a: 0 wt% (■), 0.02 wt% (□), 0.5 wt% (*), 1.4 wt% (⧗)

to give usable results, the $T_{1\rho}$ relaxation times have been investigated.

The magnetization vs. spin-lock time curves show that the relaxation is nearly monoexponential for PAc with $T_{1\rho} = 12$ ms and biexponential for PU with respectively 2 ms for the species representing 95% of the signal and 0.2 ms for the remaining 5%. This 5% may correspond to the crosslink points of PU. The relaxation of both types of IPNs, Sim and Seq, gives approximately the linear combination of the exponentials associated to the homonetworks, i.e. 75% with a relaxation time of 12 ms and 25% with 2 ms. Note that the component with 0.2 ms relaxation time does not appear, as it represents only 1% of the total relaxation.

These results, obtained from the decomposition into a sum of two exponentials, seem at first view inconsistent with the previous conclusions from f.i.d. analysis[3] which had shown that the dispersion of the two constituents in the IPNs depended upon their synthesis mode: the PAc and PU networks are more intimately mixed (at a very local scale) after a sequential preparation mode. Conversely, the values obtained for $T_{1\rho}$ indicate that no spin diffusion has taken place during the measurement time, which in turn indicates that over a range of 10 Å, the relaxation of one species has not been perturbed by that of the other.

In order to remove this ambiguity, the inverse Laplace transforms of the relaxation curves have been drawn for the homonetworks PU and PAc (*Figure 8*), and for the Sim and Seq IPNs (*Figure 9*). The distributions of the neat networks almost do not overlap, and that of the SeqIPN is broader than the SimIPN one. In particular, in *Figure 9* the peak of the polymethacrylic component is shifted more towards the fast relaxation rates for the SeqIPN. The extra area of this peak in the SeqIPN, compared with that of the SimIPN, represents the surplus of common averaged values of relaxation rates between PAc and PU. It indicates that in these regions, PU is close enough to PAc (< 10 Å) to be able to influence its relaxation by spin diffusion.

These considerations allow us to conclude that most of the interactions between PAc and PU in IPNs are on a scale greater than 10 Å, but because of the lack of

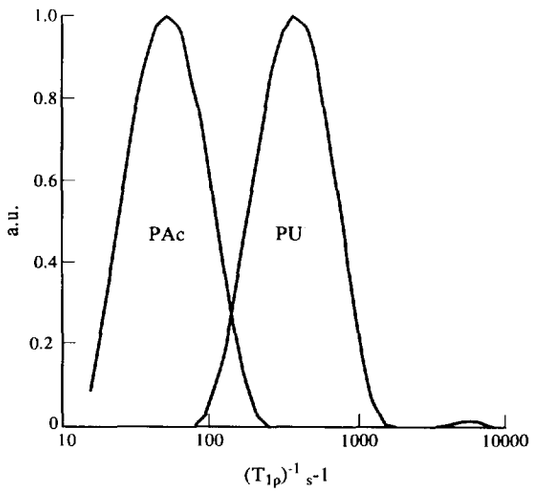

Figure 8 Distribution of spin-lattice relaxation rates in the rotating frame for PAc and PU homonetworks

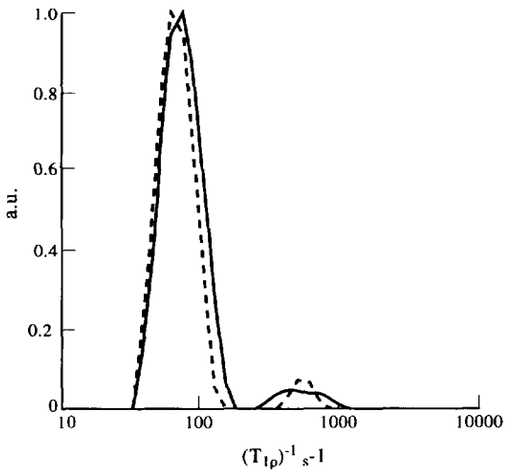

Figure 9 Distribution of spin-lattice relaxation rates in the rotating frame for SimIPN (---) and SeqIPN (———)

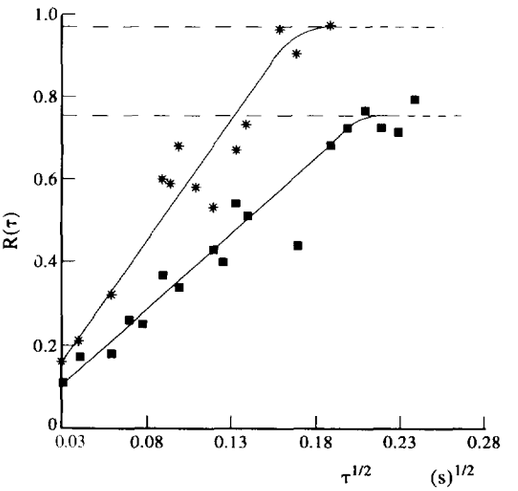

Figure 10 Recovery factor of the magnetization for PAc resonance, $R(\tau)$, in a Goldman–Shen experiment after a preparation period of 100 μs as a function of the spin diffusion time τ, for SeqIPN (*) and SimIPN (■)

information given by T_1 measurements (on a scale of about 100 Å), experiments based on the Goldman–Shen pulse sequence are necessary to obtain further detail on the structure. First, we summarize the results obtained by f.i.d. analysis[3]: three regions of different mobility have been detected. The first (50%) with a fast decay, represents PMMA (except $-O-CH_3$); the intermediate part (30–40%) is associated with the methoxy group and to the crosslink points of PU; the last, mobile part, corresponds to the elastic chains of PU. The spin–spin relaxation kinetics of these regions are characterized by a second moment of 13 G^2, and relaxation times of 21 or 22 μs and of 200–300 μs, respectively.

From these results, the value $t_0 = 100$ μs from the Goldman–Shen sequence has been chosen so that the magnetizations of the first and intermediate part have relaxed, whereas the slower relaxing spins (PU) keep part of their magnetization and may transfer it to the faster ones. *Figure 10* shows the recovery factor ($R(\tau)$) as a function of $\tau^{1/2}$ for the two types of IPNs. From the initial slope, a value of 70 Å is found for the SeqIPN. In

Figure 10 are also reported the maxima of the recovery factors. It is close to 1 for the SeqIPN, indicating that if PAc inclusions exist, they are smaller than 300 Å. Thus, considering the length of the autodiffusion path in PU (70 Å) and the maximum size of the inclusions of PAc (< 300 Å), we are able to conclude that the degree of dispersion in the SeqIPN is very high.

In the case of the SimIPN, we have found a length for the autodiffusion path in PU of 90 Å, and a recovery factor of 0.75. The difference in size (70 and 90 Å) between the two IPNs is within the limit of experimental error and therefore not significant. However, the value of the recovery factor (0.75) for the SimIPN at delays τ for which $R(\tau) = 1$ for SeqIPN indicates a structure which consists of PAc inclusions with sizes over 300 Å, because the core of the PAc inclusions cannot be reached by the magnetization transfer of PU. Note that TEM observations had shown nodule sizes of several micrometres for these SimIPNs[4], attributed to PAc alone and representing about 8% of the sample. The inclusions of pure methacrylic component (> 300 Å) corresponding to 25% of the PAc pointed out by the Goldman–Shen experiment cannot be related to the TEM inclusions. Indeed, the scales of observation of the two techniques are different. By TEM, inclusions with sizes around 300 Å are not visible, and by n.m.r. distinction between PAc inclusions of 300 Å and PAc nodules of several micrometres is not possible.

CONCLUSIONS

By SEM of chemically treated samples of PU/PS semi-1 IPNs, structures consisting of PS nodules surrounded by a highly PU-enriched shell in an homogeneous PU/PS matrix are observed. The n.m.r. results show in detail the regions which appear as the 'matrix' by SEM, and do not bring new information concerning the gross heterogeneities because domains larger than 300 Å give identical n.m.r. responses. All the samples contain PU domains larger than 300 Å, and they become bigger as the amount of PS_a increases. Furthermore, these materials may be divided into two types: in the first, containing less than 0.5 wt% PS_a, homogeneous regions exist within a range of 10 Å without PS-rich regions of sizes over 100 Å; for the other, with at least 0.5 wt% PS_a, phase separation takes place, so that pure PS domains of a size over 100 Å exist. So, on the finer n.m.r. scale, it is possible to specify the degree of mixing in the different phases.

With regard to PU/PAc IPNs, the earlier f.i.d. analysis, which showed that more local interactions exist in a sequentially synthesized IPN, is corroborated by $T_{1\rho}$ determinations.

The TEM pictures of these IPNs suggest a PU/PAc matrix containing, only for the Sim type, PAc inclusions; the n.m.r. investigations yield considerably more detail: the matrix of the Sim and Seq IPNs consists in fact of a homogeneous blend of PU and PAc domains smaller than 100 Å for both components. In the case of the Sim IPN, inclusions exist, containing a core of pure PAc larger than 300 Å; the matrix itself is richer in PU.

Finally, it is interesting to emphasize that, although the semi-1 IPNs are synthesized in the sequential mode, their morphology resembles that of SimIPNs with a given amount of PS_a: in this case, as soon as PU microgels begin to form, phase separation between the solution of highly branched PU molecules in styrene and the solution of PS in styrene is likely to occur. In the SimIPNs both species form more or less at once, which reproduces the former situation.

REFERENCES

1 Sperling, L. H. 'Interpenetrating Networks and Related Materials', Plenum Press, New York, 1981
2 Huelck, V., Thomas, D. A. and Sperling, L. H. *Macromolecules* 1972, **5**, 340, 348
3 Parizel, N., Meyer, G. C. and Weill, G. *Polymer* 1993, **34**, 2495
4 Tabka, M. T., Widmaier, J. M. and Meyer, G. C. in 'Sound and Vibration Damping with Polymers' (Eds R. D. Corsaro and L. H. Sperling), American Chemical Society, Washington, DC, 1990
5 He, X. W., Widmaier, J. M. and Meyer, G. C. *Polymer Int.* 1993, **32**, 289 (two papers)
6 Djomo, H., Morin, A., Damyanidu, M. and Meyer, G. C. *Polymer* 1983, **24**, 65
7 Whittall, K. P. *J. Magn. Reson.* 1989, 134
8 Hirschinger, J., Meurer, B. and Weill, G. *Polymer* 1987, **28**, 721
9 Provencher, S. W. *Comput. Phys. Commun.* 1982, **27**, 213
10 Provencher, S. W. *Comput. Phys. Commun.* 1982, **27**, 229
11 Goldman, M. and Shen, L. *Phys. Rev.* 1966, **144**, 321
12 Legrand, A. P. *J. Chim. Phys.* 1987, **84**, 1203
13 Lauprêtre, F. *J. Chim. Phys.* 1987, **84**, 1238
14 Assink, R. A. *Macromolecules* 1978, **11**, 1233
15 Clauss, J., Schmidt-Rohr, K. and Spiess, H. W. *Acta Polym.* 1993, **44**, 1
16 Abragam, A. and Goldman, M. in 'Nuclear Magnetism: Order and Disorder', Oxford University Press, New York, 1982
17 Douglass, D. C. and McBrierty, V. J. *Polym. Eng. Sci.* 1979, **19**, 1054
18 McBrierty, V. J. and Douglass, D. C. *Phys. Rep.* 1980, **63**, 63
19 Bloembergen, N. *Physica* 1949, **15**, 386
20 Clayden, N. J. and Howick, C. *Polymer* 1993, **34**, 2508
21 Tanaka, H. and Nishi, T. *Phys. Rev. B* 1986, **33**, 32
22 Cheung, T. T. P. and Gerstein, B. C. *J. Appl. Phys.* 1981, **52**, 5517
23 Fedotov, V. D. and Schneider, H. in 'NMR Basic Principles and Progress' (eds P. Diehl, E. Fluck, H. Gunther, R. Kosfeld and J. Seelig), Vol. 21, Springer-Verlag, Berlin, 1989